CENTRAL ASIAN JOURNAL OF MEDICAL AND NATURAL SCIENCES
https://cajmns.casjournal.org/index.php/CAJMNS
Volume: 07 Issue: 02 | April 2026 ISSN: 2660-4159

Article

Synthesis, Study the Antibacterial Activity, Molecular Docking and Liquid Crystals Properties of Some New Heterocyclic Compounds

Safana Awef Abdel Rahman*[1], Safa Mahmood Shawkat[2], Ehab Mohammed Faraj[3] ,Fawzi Hameed Jumaa[4]

1. College of Pharmacy, Tikrit University
2. Department of Chemistry, College of Science, Tikrit University.
3. Salah al-Din Education Directorate.
4. Department of Chemistry, College of Education for Women, Tikrit University.

* Correspondence: sfana.a.abdulrahman@tu.edu.iq

Abstract: This work involved the synthesis of tetrazole and Hexagonal rings, saturated and unsaturated heptagonal rings azo dye by the reaction of 4,4'-(diazene-1,2-diyl)di aniline with aldehyde group synthesis of Schiff base (S1) in ethanol through the reaction of the substituted amine in THF as a solvent, with sodium azide and synthesis of by reacting Schiff bases with amino benzoic acid to prepare 2,3-dihydroquinazoline 4-one prepared with absolute ethanol as a solvent and using sodium bicarbonate, and preparing 1,3oxazepane4,7-dione through the reaction of succinic anhydride with new Schiff bases, and preparing 1,3oxazepen4,7-dione from During its reaction with maleic anhydride in the existence of dry benzene as a solvent. FT- IR,13CNMR and 1H-NMR Spectrophotometric methods were used to characterize the prepared compounds, the antibacterial activity

Keywords: Tetrazole, prepare 2,3-dihydroquinazoline 4-one, 1,3-Oxazepine, 1,3-oxazepane, Molecular docking, Liquid crystal.

Citation: Rahman, S. A. A, Shawkat, S. M, Faraj, E. M & Jumaa, F. H. Synthesis, Study the Antibacterial Activity, Molecular Docking and Liquid Crystals Properties of Some New Heterocyclic Compounds. Central Asian Journal of Medical and Natural Science 2026, 7(2), 389-408.

Received: 10th Dec 2025
Revised: 21th Jan 2026
Accepted: 04th Feb 2026
Published: 22th Mar 2026

1. Introduction

Schiff bases are organic compounds defined by the azomethine group (-C=N-) [1, 2]. Also known as imines, they are specifically called aldimines when derived from aldehydes and ketimines when derived from ketones [3]. They are typically synthesized via the condensation of an aldehyde or ketone with an amine. Classical methods, like the Staabe preparation, use azeotropic distillation with benzene to remove water (4). A more common approach is refluxing equimolar amounts of reactants, followed by purification via recrystallization [4]. Schiff bases are vital in diverse scientific fields [5] and biological processes, including non-enzymatic transamination and vitamin B6-catalyzed reactions [6]. Many also exhibit significant pharmacological activities, such as anticancer effects [7]. Tetrazoles are five-membered heterocyclic rings containing one carbon and four nitrogen atoms [1, 2]. They exist as three parent isomers (1H-, 2H-, and 5H-tetrazole) based on double bond positions [8]. Despite industrial uses as catalysts and explosives [9], their unique electronic properties make them valuable in medicinal chemistry, demonstrating a wide spectrum of activity including anti-inflammatory, analgesic, anticancer, anticonvulsant, and antiviral effects (9).Hydro quinazoline compounds are pharmacologically significant, featuring in numerous drugs and antimicrobials [10].

In particular, 1,2-dihydroquinazoline derivatives serve as insecticides, antibacterial agents, and exhibit anti-inflammatory, sedative, anti-apoptotic, and CNS activities [11]. Oxazepanes are seven-membered heterocycles with five carbons, one nitrogen, and one oxygen [12]. They are often synthesized via cycloaddition to a Schiff base's azomethine group [13] and have three main isomers (1,2-, 1,3-, and 1,4-oxazepane) [14]. Their biological importance is highlighted by their antiviral, anticonvulsant, and antimicrobial properties [15-17]. Similarly, oxazepines are seven-membered, non-aromatic heterocycles with the same atomic composition but distinct isomeric forms (1,2-, 1,3-, and 1,4-oxazepine) based on heteroatom numbering [18]. Their seven-membered ring structure is non-planar, adopting a boat-like conformation, which accounts for their lack of aromaticity [19]. Molecular docking is a fundamental computational tool in structural biology and drug design. It predicts the preferred orientation of a ligand when bound to a target protein, based on geometric and chemical complementarity [20]. Its primary goal is to predict interaction, identify the most stable binding conformation at an enzyme's active site (lowest energy), and estimate binding affinity [21]. Liquid crystals are a distinct state of matter with properties intermediate between crystalline solids and isotropic liquids. First observed in 1888 by Reinitzer, cholesteryl benzoate exhibited two melting points: it transformed into a turbid liquid at 146°C and became clear (isotropic) at 179°C. This transition is reversible upon cooling [22].

2. Materials and Methods

2.1. Material

All chemicals used in this work were of analytical grade and purchased from commercial suppliers, including Fluka, Aldrich, and BDH. They were used without further purification unless otherwise stated. Solvents such as ethanol, tetrahydrofuran (THF), benzene, and 1,4-dioxane were of high purity and used as received.

2.2. Apparatus

Melting points were determined using an SMP40 automatic melting point apparatus, and the values obtained were used without correction. For thin-layer chromatography (TLC), pre-coated polygram silica gel sheets served as the stationary phase, and the spots were visualized by exposure to iodine vapor. Infrared (IR) spectra were recorded on a FT-IR-600, with samples prepared as KBr discs, over a spectral range of 400–4000 cm^{-1}. The nuclear magnetic resonance ^{1}H,^{13}C NMR spectra were measured for the compounds prepared in the laboratories of Sannati Sharif University - Iran, using MS5973 Agilent Technology, Germany Bruker 500 MHz, at 500 MHz, and using (DMSO-d^{6}) as a solvent.

2.3. Synthesis of compounds

2.3.1 Synthesis of Schiff Bases derivatives (S_1)

The Schiff base derivatives (S_1) were synthesized following previously reported procedures [23- 26]. Their physical characteristics are summarized in **Table 1**.

2.3.2. Synthesis of tetrazole (S_2) [27, 28]

Sodium azide (0.26 g, 0.001 mol) was added to a solution containing 0.002mol of the prepared Schiff base (S1) dissolved in 30 mL of THF. The resulting mixture was heated under reflux in a water bath at 80 °C for 10 h. Following the reaction, the solid product was collected by filtration and subsequently purified by recrystallization using ethanol.

2.3.3 Synthesis of 2-3,2-dihydroquinazoline-4-one compound (S_3) [29]

Mix 0.01 mol, 1.37 g of -2-aminobenzoic acid (anthranilic acid) with 0.005 mol of prepared Schiff bases (S_1) in 45 mL of abs.ethanol and 3 mL of triethylamine, then themixture was reflux for 9-15 h, then the solvent was evaporated and treated with a solution of 10% acidic sodium bicarbonate. The finalizing of the reaction was stressed using the TLC technique. Then it was filtered and recrystallized with tetrahydrofuran.

2.3.4. Synthesis of 1,3-oxazan-7,4-dione compound (S_4) [30, 31]

Mix 0.005 mol of prepared Schiff bases (S_1) in 40 mL of dry benzene with 0.01 mol, 1 g of succinic anhydride, then the mixture was heated for 11 h in a water bath, and was confirmed. After the reaction was completed using the TLC technique, the mixture was then cooled in an ice bath, the precipitate was filtered, dried, and recrystallized in 1,4-dioxane.

2.3.5. Synthesis of 1,3-oxazpine-7,4-dione compound (S_5) [32, 33]

Mix (0.005 mol) of prepared Schiff bases (S_1) in 40 ml of dry benzene with (0.01 mol, 1.0g) of maleic anhydride, then the mixture was reflux for 12h in a water bath, and was confirmed. After the reaction was completed using the TLCtechnique, the mixture was then cooled in an ice bath, the precipitate was filtered, dried, and recrystallized in 1,4-dioxane.

Table 1. physical of prepared compounds(S_1-S_5).

No	Mole. Formula	M.wt g/mole	M.P.	Time(h)	Color	yield%	R.F
S_1	$C_{30}H_{24}N_6O_2$	501.2	270-272	9	Orange	84	0.73
S_2	$C_{30}H_{26}N_{12}O_2$	586.607	290-292	10	Deep Yellow	84	0.83
S_3	$C_{36}H_{26}N_6O_6$	638.628	274-276	15	Deep Yellow	62	0.82
S_4	$C_{38}H_{30}N_6O_8$	698.69	275-277	11	Light Brown	63	0.84
S_5	$C_{44}H_{34}N_8O_4$	738.8052	261-269	12	Green	95	0.78

2.4. Biological Activity Study

The antibacterial activity of the synthesized compounds was evaluated in vitro against two pathogenic bacterial strains: Gram-positive Staphylococcus aureus and Gram-negative Pseudomonas aeruginosa, using the agar well diffusion method. Mueller-Hinton agar was prepared by suspending the medium in distilled water (1 L), heating with continuous stirring using a magnetic stirrer until complete dissolution, and then sterilizing by autoclaving at 121 °C and 1.5 bar for 2 h. The sterile medium was cooled to approximately 50 °C, poured into sterile Petri dishes, and allowed to solidify at room temperature. Bacterial isolates were obtained from pure cultures and moved from the solid medium to test tubes containing 5 mL of sterile dist. water using heat-sterilized loops. The suspensions were incubated at 37 °C for 16 h. Subsequently, the cultures were diluted with sterile physiological saline solution until the turbidity matched the 0.5 McFarland standard, corresponding to a bacterial cell concentration of approximately 1.5×10^8 colony-forming units (CFU)/mL. Stock solutions of the synthesized compounds (S_1–S_5) were prepared by dissolving0.1 g of each compound in 10mL of dimethyl sulfoxide (DMSO) to obtain a concentration of 10 mg/mL. From this stock, three working concentrations (25, 50, and 75 mg/mL) were prepared by appropriate dilution with DMSO. For the agar well diffusion assay, the surface of the inoculated agar plates was punched with a sterile cork borer to create wells (6–8 mm in diameter). Aliquots (100 µL) of each compound at the prepared concentrations were introduced into the wells. The plates were incubated at 37 °C for 24 h. Antibacterialactivity was assessed by measuring the diameter of the inhibition zones (including the well diameter) in millimeters. DMSO was utilized as a negative control, while ampicillin and amoxicillin were employed as positive reference standards. All experiments were performed in triplicate, and the results were recorded as mean values.

2.5. Molecular docking study of some prepared compounds [34]

To gain insight into the possible binding modes and mechanisms of action of the synthesized compounds, a molecular-docking eximation was conducted using the AutoDock Vina software package. The three-dimensional structures of the target proteins, S. aureus (PDB ID: 3OZB) and P. aeruginosa (PDB ID: 4DQ2), were obtained from the RCSB Protein Data Bank (www.rcsb.org). The ligands (S_1–S_5) were drawn utilized Chem-draw Professional 16.0 and energy-minimized using the MM2 force field in Chem3D 16.0. Prior to docking, the protein structures were processed by deleting water molecules,

adding polar hydrogens, and applying Kollman united atom charges. The protein structures were processed by deleting water molecules, adding polar hydrogens, and applying Kollman united atom charges. using Auto Dock Tools. The prepared ligands and proteins were saved in PDBQT format. Molecular docking calculations were conducted within a grid box that was positioned to cover the binding site of each target protein. The observed binding interactions between the ligand and protein included both hydrogen-bonds and hydrophobic contacts, were analyzed and visualized utilizing discovery studio 2020 Client.

3. Results and Discussion

The study included the synthesis of Schiff bases(S_1) and tetrazole(S_2)and 2-3,2-dihydroquinazoline-4-one derivatives and of 1,3-oxazan-7,4-dione derivatives and of 1,3-oxazan-7,4-dione derivatives as in (**Scheme 1**) and spectro-methods such as FT-IR , ^{1}H-NMR and ^{13}CNMR were used to validate the structure of synthesized compounds

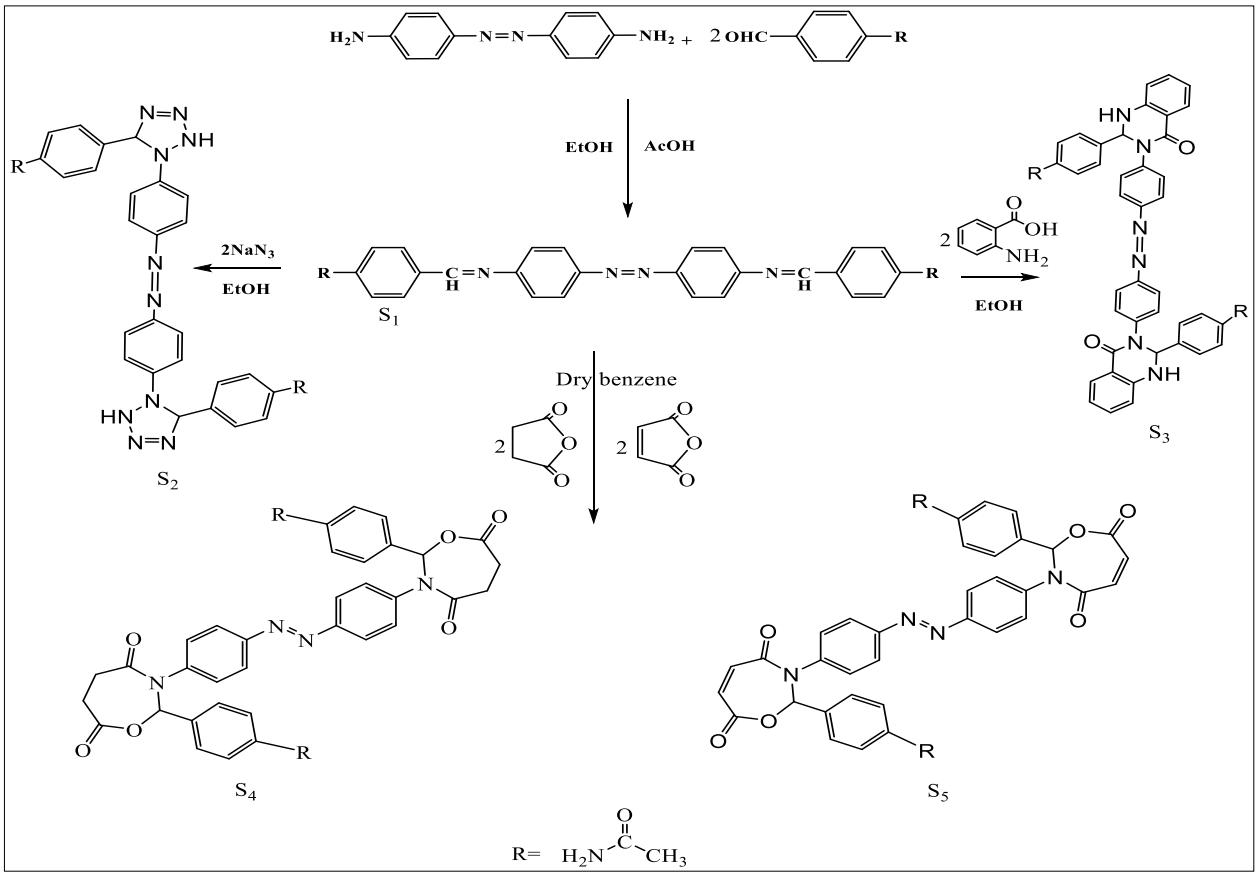

Scheme 1. Prepared comp. (S1-S5)

3.1. Characterization of compounds

3.1.1. Characterization of Schiff base (S_1)

Orange crystalline solid . FT-IR (cm^{-1}): 3276 (NH) 3047 (C-H arom.), 2962-2914 (CH arom.) 1662 (C=O), 1573 (C=N), 1529 (C=C); ^{1}H NMR (500MHz,DMSO, δ, ppm): 10.09 (1H, s, NH), 8.26 (1H,s,H-C=N), 7.7-7.6 (4H, dd, J=3.5 Hz, Ar=N-), 7.5-7.3 (4H,dd, J=4Hz , Ar-CH), 2.14 (6H, s,CH3) ; ^{13}CNMR (500 MHz, DMSO) δ 168.85(C=O), 162.19(Ph-C=N), 151.39, 149.30, 140.27, 133.59,130.08, 137.37,125.24, 123.33, 122.36, 120.49, 117.38 (C arom.), 21.63 (CH3). As shown in Figures 1, 2 and 3.

3.1.2. Characterization of Tetrazole (S_2)

Deep Yellow crystalline solid . FT-IR (cm^{-1}): 3276 (NH),3041 (C-H arom.), 2929-2867 (CH aliph.) 1660 (C=O), 1525 (C=C); ^{1}H NMR (500MHz,DMSO, δ,ppm): 11.84 (2H, s, NH), 7. 87-7.62 (4H, dd, J=4.3Hz, Ar=N-), 7.57-7.51 (4H,dd, J=3.8Hz , Ar-CH), 5.44 (2H, s, NH),

2.28(2H, s,CH) 2.14 (6H, s,CH3) ; ^{13}CNMR (500 MHz, DMSO) δ 168(C=O), 143.47, 141.92, 138.00, 129.60,125.86, 125.06,1240.10, 115.25, (C arom.), 101.75 (CH), 21.16(CH3). As shown in Figure 4.

3.1.3. Characterization of di hydro quinazoline (S3)

Deep Yellow crystalline solid . FT-IR (cm^{-1}): 3325 (NH) 3055 (C-H arom.), 2929-2856 (CH aliph.) 1664 and 1608 (C=O), 1523 (C=C); ^{1}H NMR (500MHz,DMSO, δ,ppm): 9.92 (2H, s, NH), 8.01-7.73 (6H, dd, J=5.4 ,Hz, Ar=N-), 7.70-7.54 (4H,dd, J=3.6Hz , Ar-CH), 7.49-7.12(4H,dd, J=4.8Hz , Ar-CH), 6.38 (2H, s, NH), 6.06 (2H, s,CH) 2.14 (6H, s,CH3) ; ^{13}CNMR (500 MHz, DMSO) δ 168.84 and 163.93 (C=O), 152.10, 148.40, 145.58, 141.43,139.06, 137.95,134.76, 130.36, 127.90, 127.80, 125.50, 122.88, 122.67,120.17, 115.73,113.65(C arom.), 82.30 (CH). 22.89(CH3). As shown in Figures 5, 6 and 7.

3.1.4. Characterization of Oxazepane (S4)

Light Brown crystalline solid . FT-IR (cm^{-1}): 3272 (NH) 3062 (C-H arom.), 2920-2867 (CH aliph.) 1733 and 1662 (C=O), 1527 (C=C); ^{1}H NMR (500MHz,DMSO, δ, ppm): 9.72 (2H, s, NH), 8.24-8.723 (4H, dd, J=5, 5 Hz, Ar=N-), 7.63-7.61 (4H,dd, J=6Hz, Ar-CH), 7.52-7.39(4H,dd, J=5.5Hz , Ar-CH), 2.72-2.68 (4H, t, J=3.5Hz, CH2), 2.65-2.61 (4H, t ,J=3Hz, CH2) 2.14 (6H, s,CH3) ; ^{13}CNMR (500 MHz, DMSO) δ 172.74 , 171.40 and 168.84 (C=O), 143.47, 138.12, 137.11, 133.44,130.36, 128.53,125.50, 121.48, 121.01, 127.80, 125.50, 122.88, 122.67,120.17, 115.73,113.65(C arom.), 87.47 (CH), 31.72, 27.30(CH2), 20.69(CH3) . As shown in Figures 8, 9 and 10.

3.1.5. Characterization of Oxazepine (S$_5$)

Green crystalline solid . FT-IR (cm^{-1}): 3303 (NH) 3049 (C-H arom.), 2993-2916 (CH aliph.) 1731 and 1627 (C=O), 1554 (C=C); ^{1}H NMR (500MHz,DMSO, δ, ppm): 9.83 (2H, s, NH), 8.07-8.06 (2H, dd, J=4.3,Hz, Ar=N-),7.88 (2H,s,CH) 7.68-7.66(2H,dd, J=5.2Hz, Ar-CH), 7.60-7.42(4H,dd, J=4.5, 5Hz , Ar-CH), 6.87-6.37 (4H, d, J=3 , 3.8Hz, CH), 2.14 (6H, s,CH3) ; ^{13}CNMR (500 MHz, DMSO) δ 168.84 , 165.76 and 157.54 (C=O), 149.66, 143.47, 138.17, 138.17,132.98, 132.96,128.55, 125.51, 124.64, 123.03, 121.43, 121.43, 121.01 (C arom.), 94.90 (CH), 21.63(CH3) . As shown in Figures 11, 12 and 13.

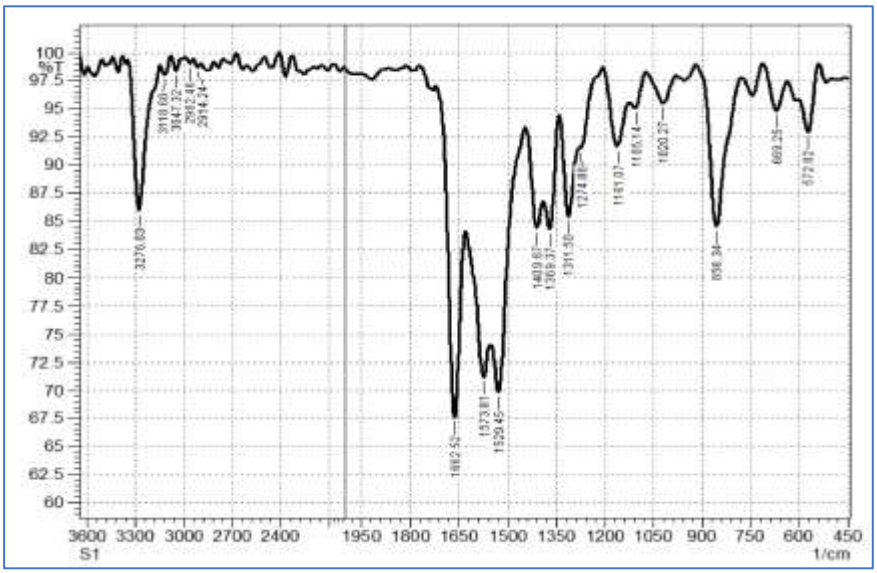

Figure 1. FT-IR spectrum of comp.(S$_1$)

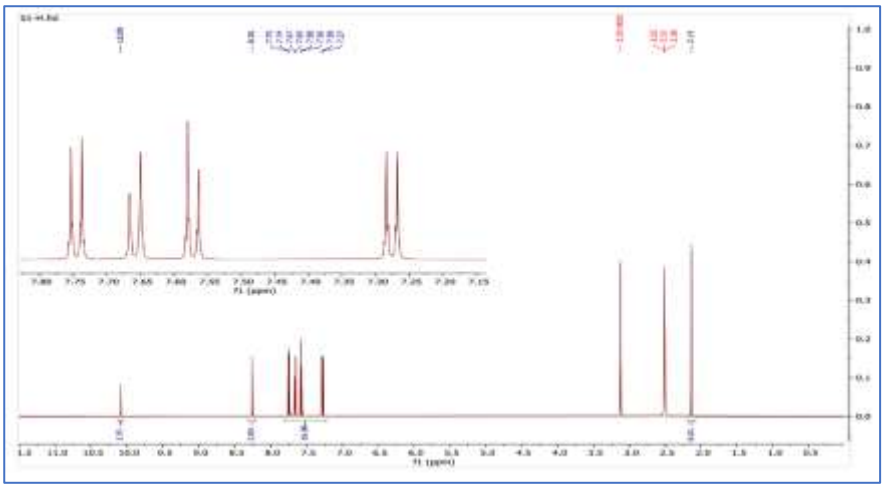

Figure 2. ^{1}H NMR spectrum of comp. (S_1)

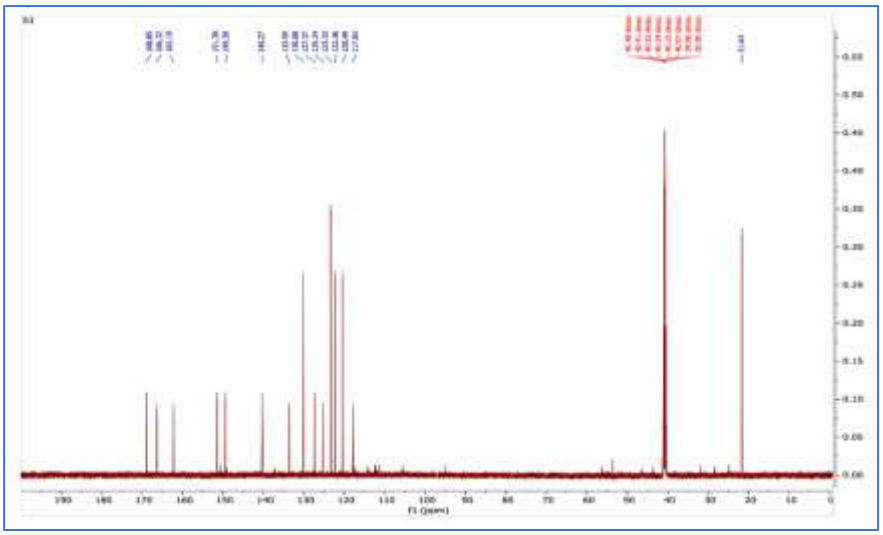

Figure 3. ^{13}C NMR spectrum of comp. (S_1)

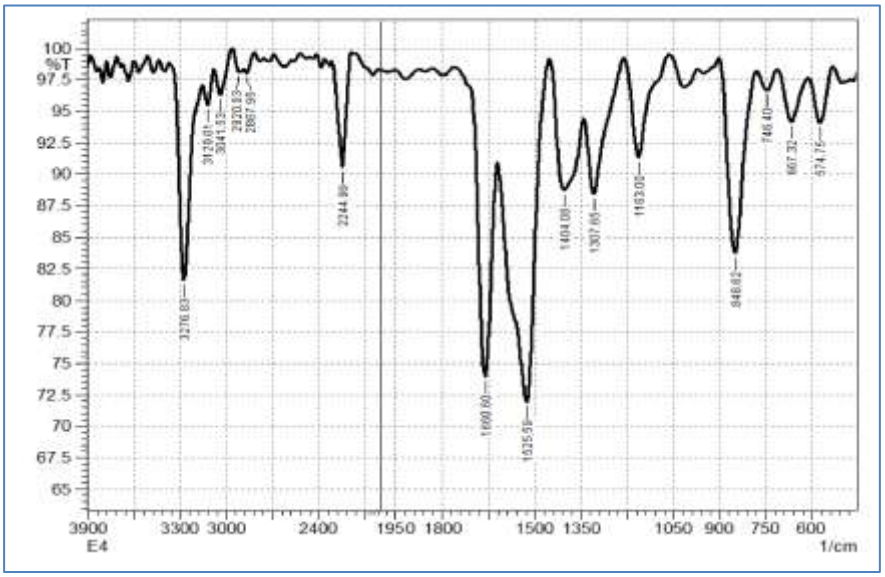

Figure 4. FT-IR spectrum of comp.(S_2)

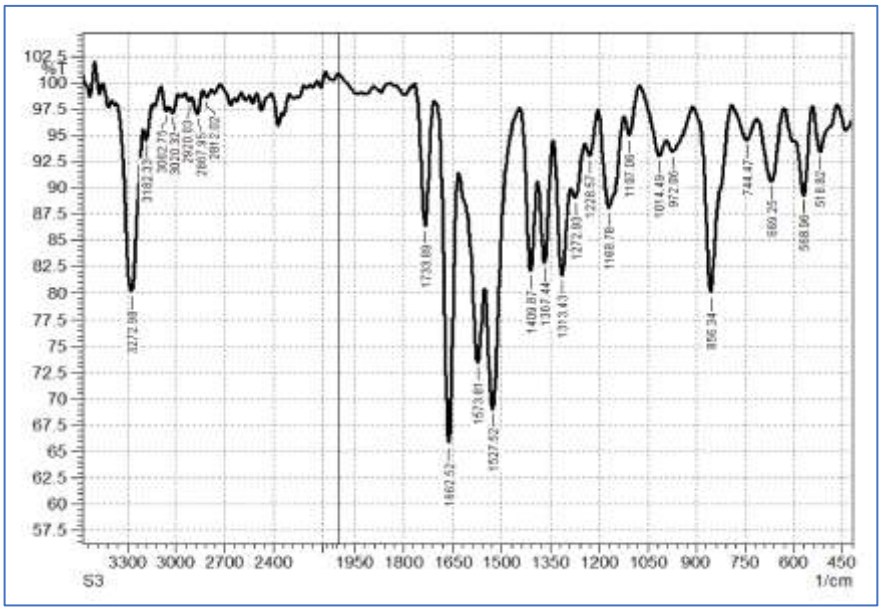

Figure 5. FT-IR spectrum of comp.(S_3)

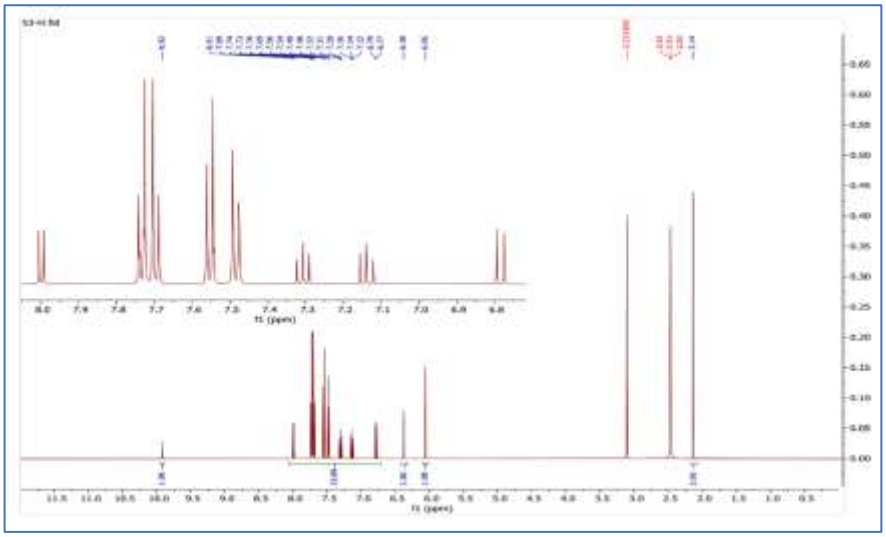

Figure 6. ^{1}H NMR spectrum of comp. (S_3)

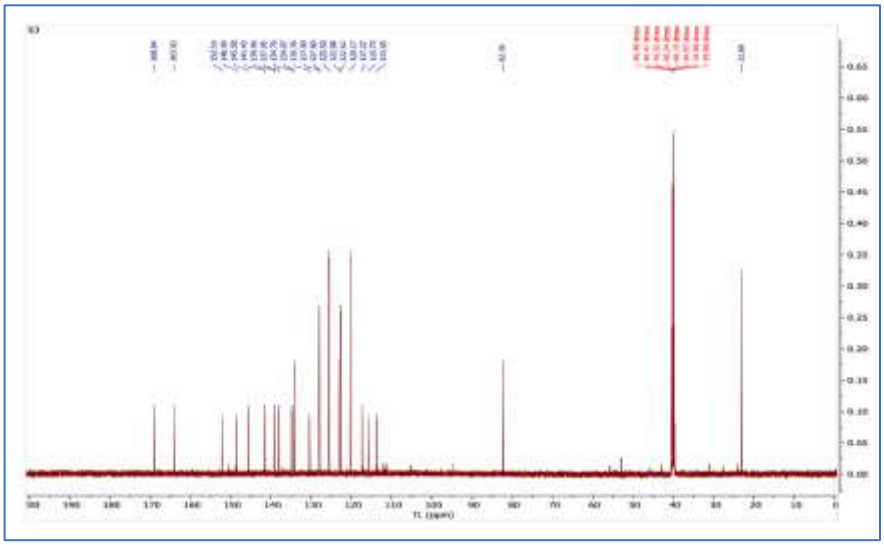

Figure 7: ^{13}C NMR spectrum of comp. (S_3)

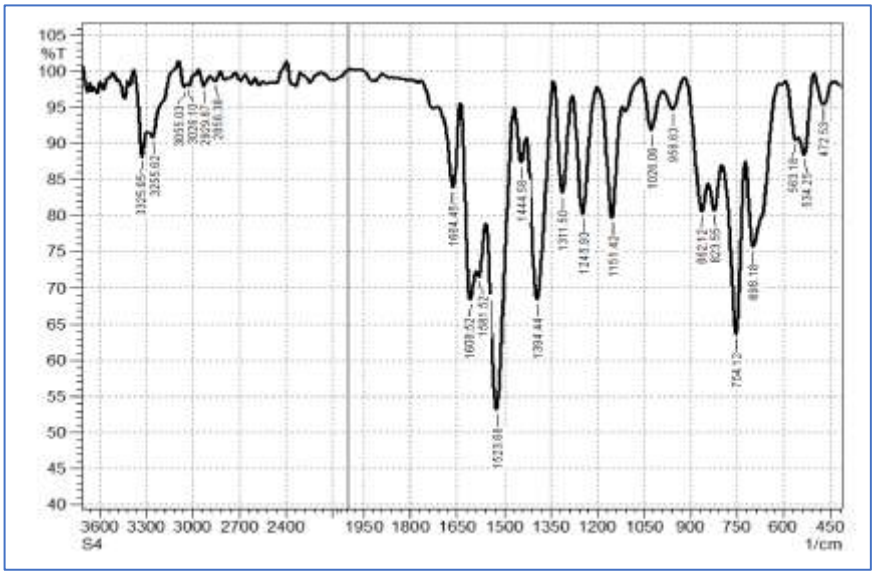

Figure 8. FT-IR spectrum of comp.(S_4)

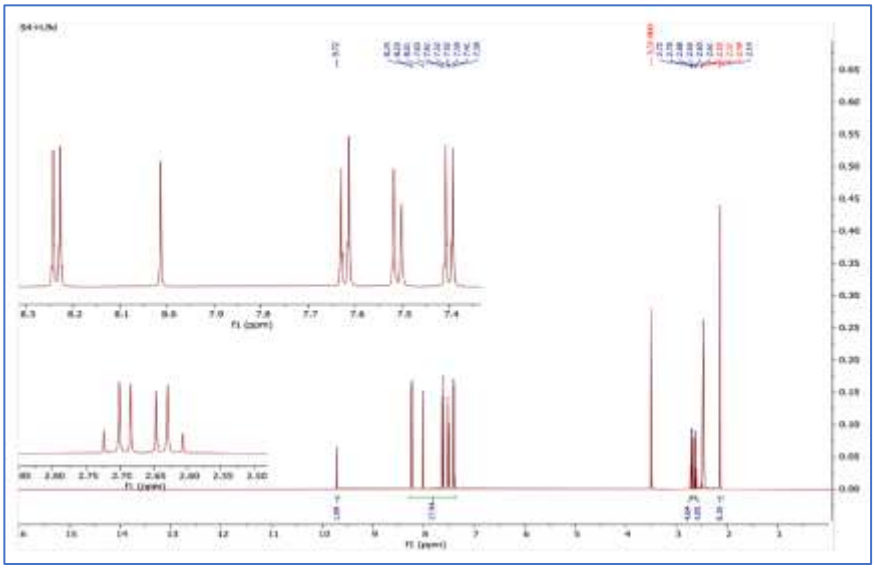

Figure 9. ^{1}H NMR spectrum of comp.(S_4)

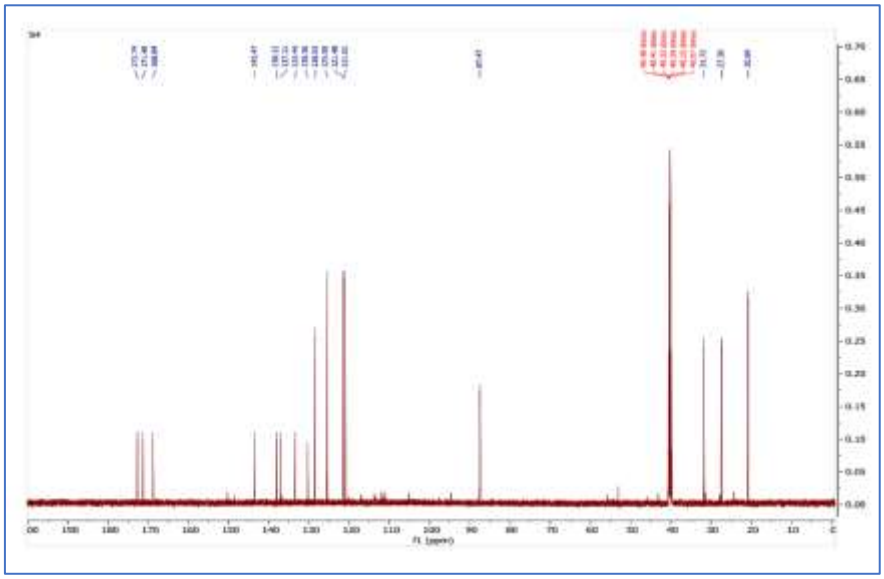

Figure 10. ^{13}C NMR spectrum of comp. (S_4)

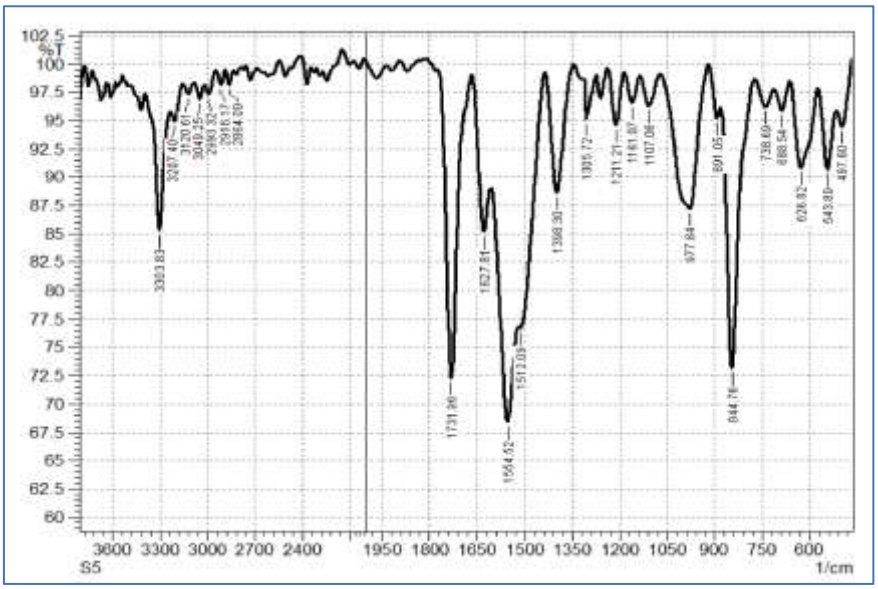

Figure 11. FT-IR spectrum of comp.(S_5)

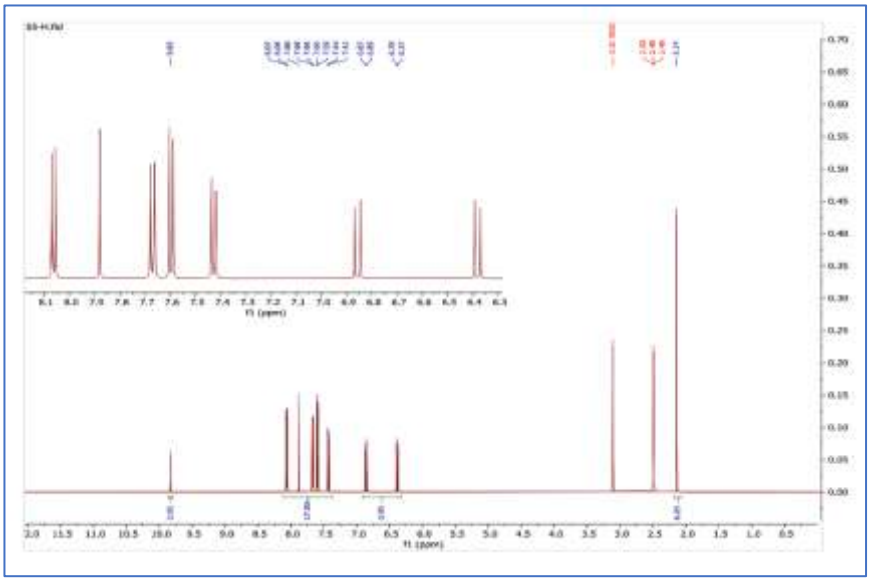

Figure 12. ^{1}H NMR spectrum of comp.(S_5)

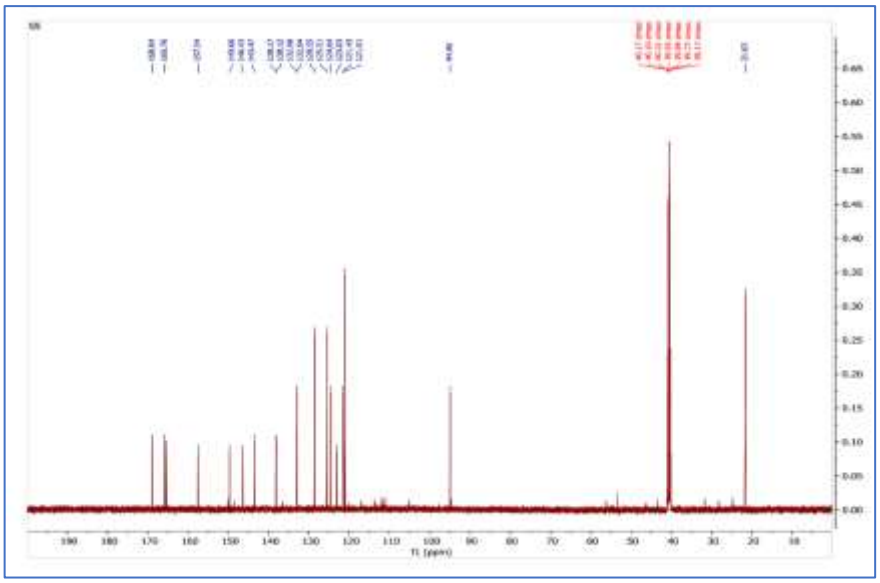

Figure 13. ^{13}C NMR spectrum of comp. (S_5)

3.2. Assessment of Biological Activities

Due of their widespread disease-causing ability, these bacteria were chosen for medical research. They also range in how resistant they are to drugs. Methods like drilling and sample testing were used to assess the bioavailability for some of the synthesized compounds. The findings demonstrated that the synthesized compounds may stop the growth of various concentrations of the Gram stain-using antibiotics ampicillin and amoxicillin. Control samples and these antibiotics are widely classified, specifically these two types, in addition to many types, based on what the Ministry of Health laboratories and World Health Organization tests use. They also have a large inhibitory diameter due to their high selectivity when studying the susceptibility of bacteria to the prepared compounds. Compound (S_3) showed good inhibition effect against Pseudomonas aeruginosa, and the inhibition diameter was (5 cm), while compound (S_5) showed good inhibitory activity against Staphylococcus aureus with an inhibition rate of (5 cm). Percentage, the concentration is directly related to inhibition, the higher the concentration, the higher the inhibition rate [35-37], as shown in Table 2 and Figures 14-17.

Table 2. Antibacterial Activity of the Prepared Compounds Against Pseudomonas aeruginosa and Staphylococcus aureus

Comp. No.	Conc. mg/ml	*Pseudomonas aeruginosa*	*Staphylococcus aureus*
	$1x10^{-3}$	-	-
S_1	$1x10^{-2}$	+	-
	$1x10^{-1}$	++	+
	$1x10^{-3}$	-	+
S_2	$1x10^{-2}$	-	+
	$1x10^{-1}$	++	+
	$1x10^{-3}$	-	+
S_3	$1x10^{-2}$	+	+
	$1x10^{-1}$	+	++
	$1x10^{-3}$	-	+
S_4	$1x10^{-2}$	-	+
	$1x10^{-1}$	+	++
	$1x10^{-3}$	+	-
S_5	$1x10^{-2}$	+	+
	$1x10^{-1}$	++	++

(–) No inhibition, (+) Inhibition zone diameter 1–2 cm, (++) Inhibition zone diameter 2–4 cm

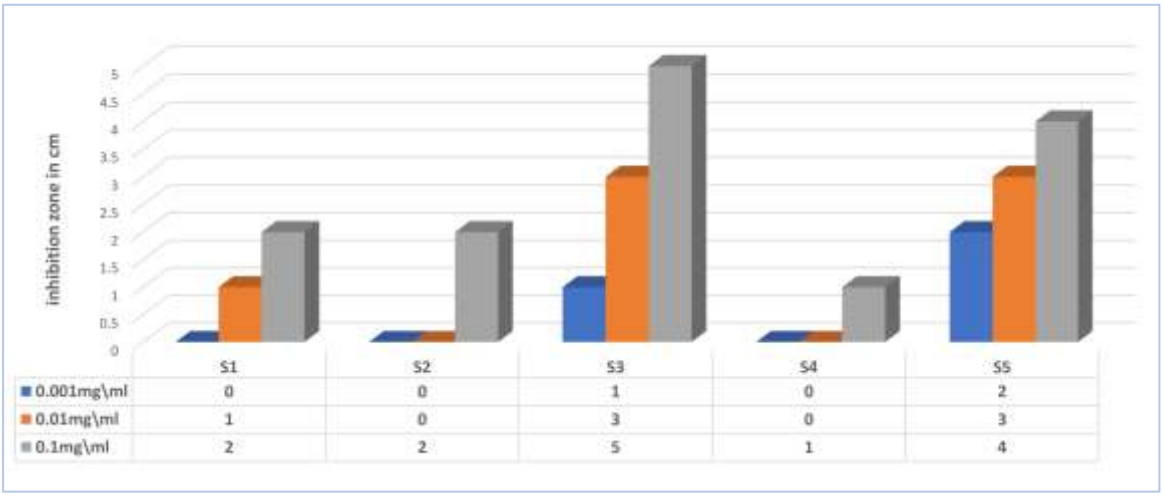

Figure 14. Inhibitory activity values of (S_1-S_5) against *Pseudomonas aeruginosa bacteria.*

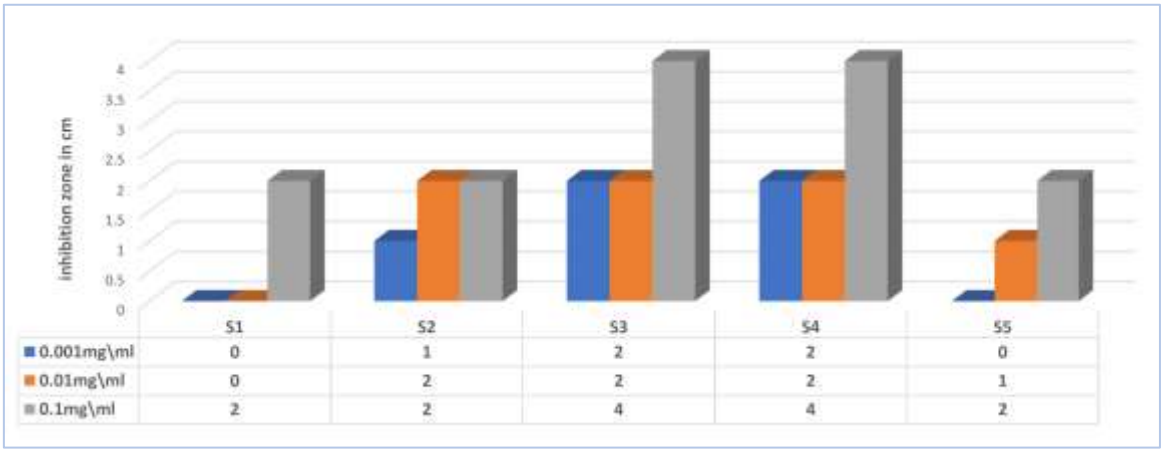

	S1	S2	S3	S4	S5
0.001mg\ml	0	1	2	2	0
0.01mg\ml	0	2	2	2	1
0.1mg\ml	2	2	4	4	2

Figure 15. Inhibitory activity values of (S_1-S_5)against *Staphylococcus aureus* bacteria

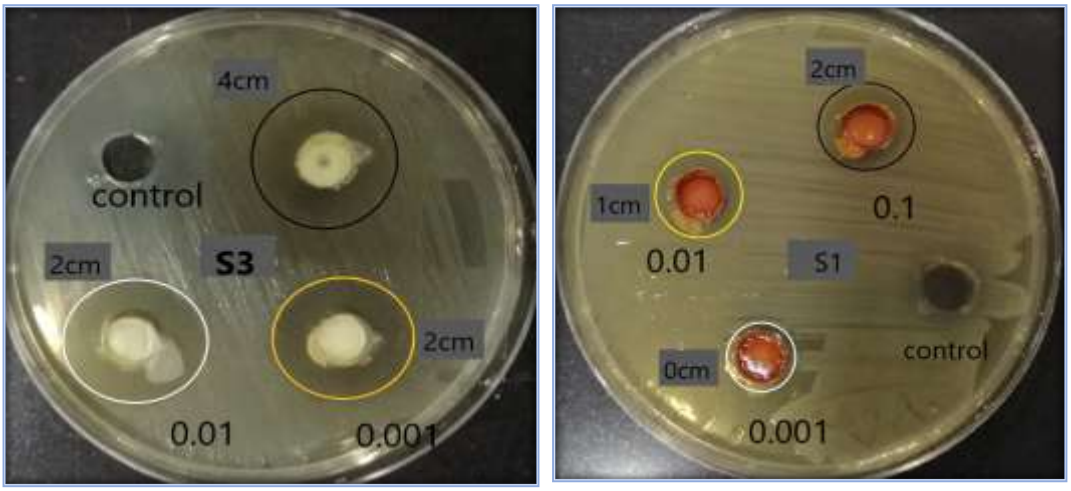

Figure 6. Efficacy of compound (S_3) Antibacterial *Staphylococcus aureus*

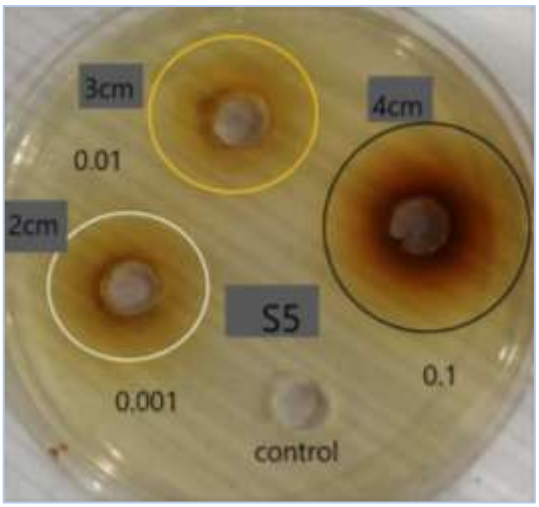

Figure 17. Efficacy of compound (S_1-S_5) Antibacterial *Pseudomonas aeruginosa*

3.3. Evaluation of Antibacterial Activity of Control Antibiotics

The results of the control antibiotics are summarized in Table 3, showing the inhibition zone diameters of Amoxicillin, Ampicillin, and Ciprofloxacin against Pseudomonas aeruginosa and Staphylococcus aureus, with the blank disk serving as a negative control.

Table 3. Antibacterial activity of control antibiotics

No.	Name	Conc. (mg/mL)	*Pseudomonas aeruginosa* (mm)	*Staphylococcus aureus* (mm)
1	Amoxicillin	1×10^{-3}	16	19
2	Ampicillin	1×10^{-3}	15	10
3	Ciprofloxacin	1×10^{-3}	12	11
4	Blank disk	—	0	0

3.4. Molecular Docking Results

To rationalize the observed antibacterial activity and gain insights into the potential binding mechanisms, molecular docking studies were performed for all synthesized compounds (S_1–S_5) within the active sites of target proteins from Staphylococcus aureus (PDB ID: 3OZB) and Pseudomonas aeruginosa (PDB ID: 4DQ2). The two-dimensional (2D) and three-dimensional (3D) interaction diagrams of the docked complexes are presented in Figures 18–26. The docking results with the S. aureus protein (3OZB) are illustrated in Figures 18–22. Specifically, Figure 18 shows the 2D and 3D interactions of compound S_1, Figure 19 corresponds to S_2, Figure 20 to S_3, Figure 21 to S_4, and Figure 22 to S_5. Similarly, the interactions with the P. aeruginosa protein (4DQ2) are depicted in Figures 23–26: S_1 (Figure 23), S_2 (Figure 24), S_3 (Figure 25), and S_5 (Figure 26). Analysis of the docking poses revealed that all compounds formed stable complexes within the active sites of both proteins through a combination of non-covalent interactions, including hydrogen bonding, π–π stacking, and hydrophobic contacts with key amino acid residues. The calculated binding energies correlated with the in vitro antibacterial activity results. Compound S_3 showed the strongest interaction against P. aeruginosa, while S_5 exhibited the most favorable binding with S. aureus, as indicated by their lower binding energy values. These findings suggest that the synthesized compounds may exert antibacterial effects through binding and possible inhibition of essential bacterial enzymes. The agreement between computational and experimental results supports the proposed binding modes and provides a basis for further structural modification.

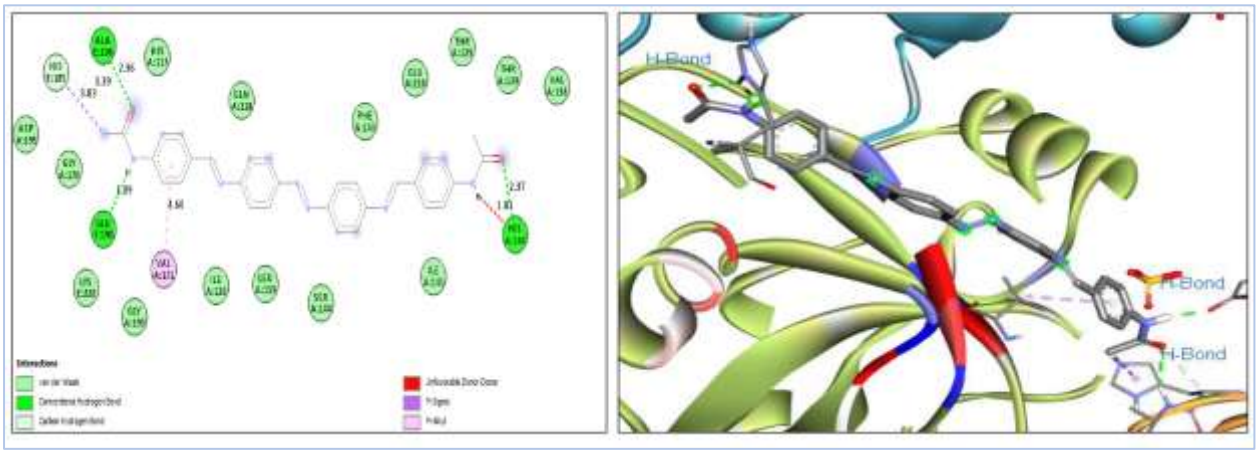

Figure 18. Three-dimensional (3D, right) and two-dimensional (2D, left) interaction diagrams of compound S_1 docked into the active site of *Staphylococcus aureus* protein (PDB ID: 3OZB).

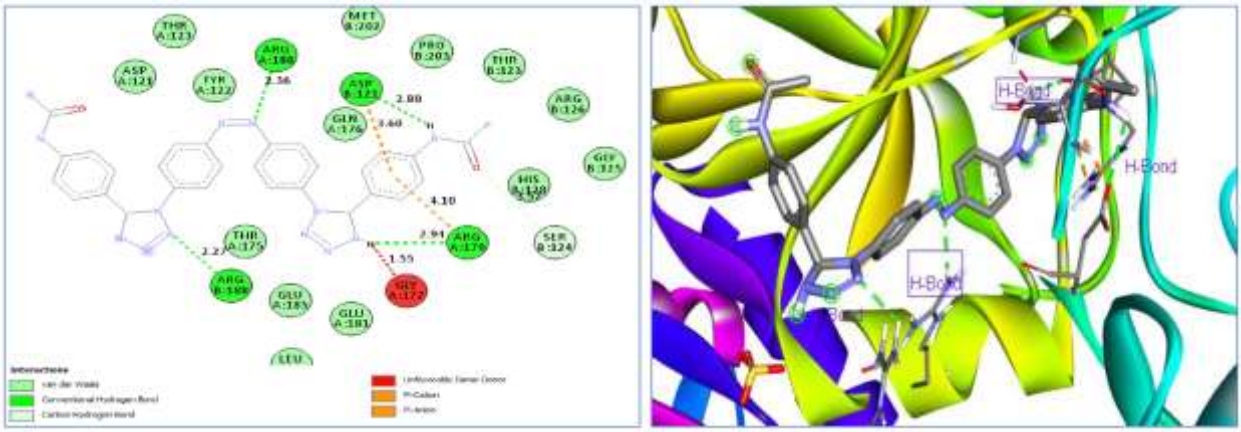

Figure 19. Three-dimensional (3D, right) and two-dimensional (2D, left) interaction diagrams of compound S_2 docked into the active site of *Staphylococcus aureus* protein (PDB ID: 3OZB).

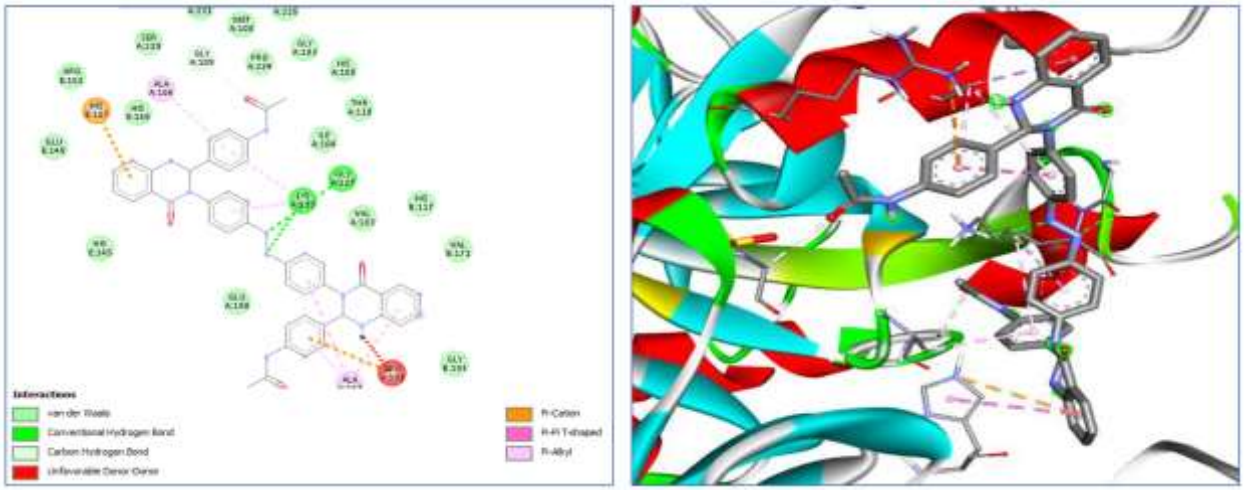

Figure 20. Three-dimensional (3D, right) and two-dimensional (2D, left) interaction diagrams of compound S_3 docked into the active site of *Staphylococcus aureus* protein (PDB ID: 3OZB).

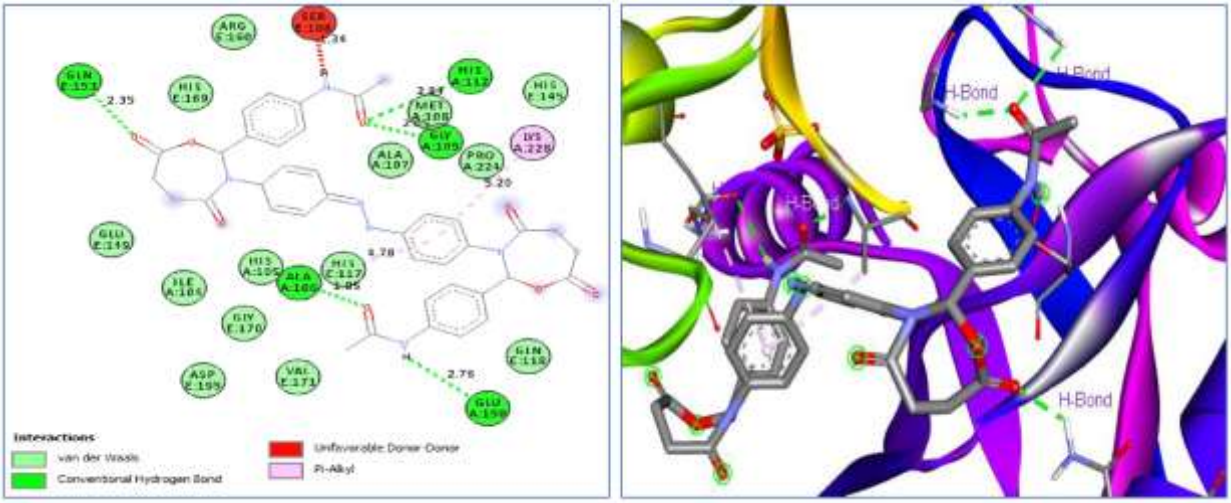

Figure 21. Three-dimensional (3D, right) and two-dimensional (2D, left) interaction diagrams of compound S_4 docked into the active site of *Staphylococcus aureus* protein (PDB ID: 3OZB).

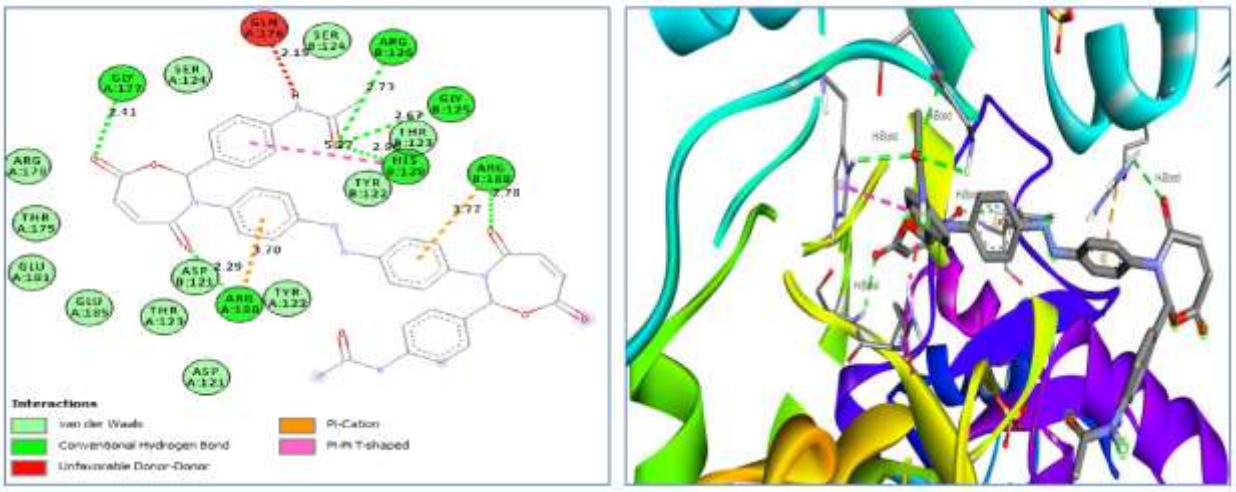

Figure 22. Three-dimensional (3D, right) and two-dimensional (2D, left) interaction diagrams of compound S_5 docked into the active site of *Staphylococcus aureus* protein (PDB ID: 3OZB).

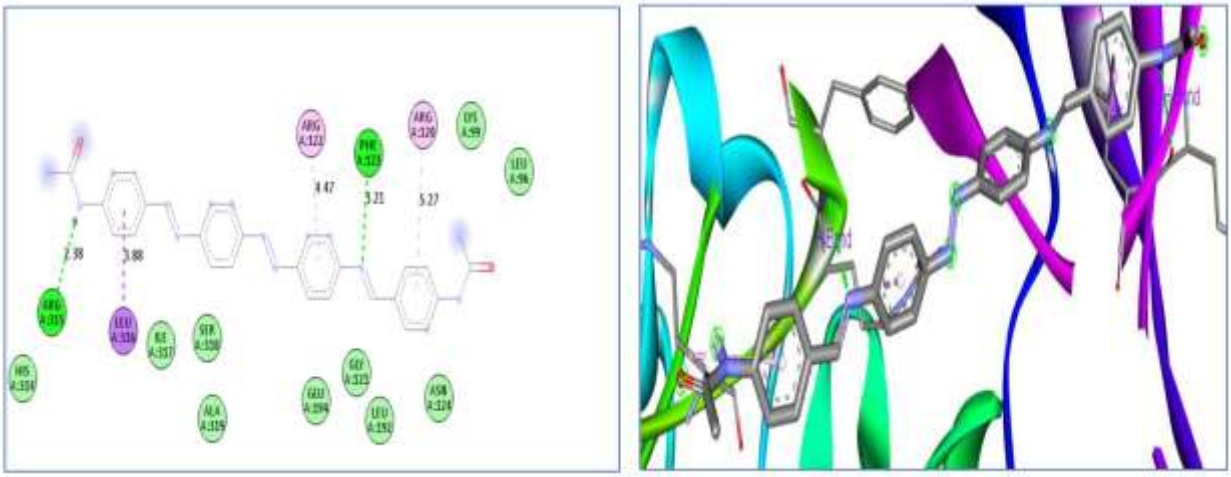

Figure 23. Three-dimensional (3D, right) and two-dimensional (2D, left) interaction diagrams of compound S_1 docked into the active site of *Pseudomonas aeruginosa* protein (PDB ID: 4DQ2).

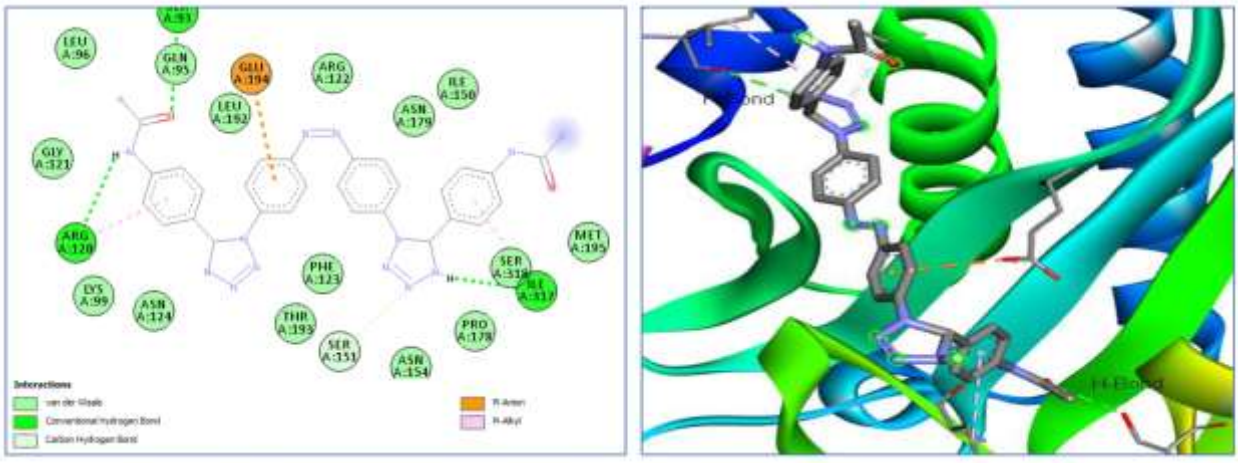

Figure 24. Three-dimensional (3D, right) and two-dimensional (2D, left) interaction diagrams of compound S_2 docked into the active site of *Pseudomonas aeruginosa* protein (PDB ID: 4DQ2).

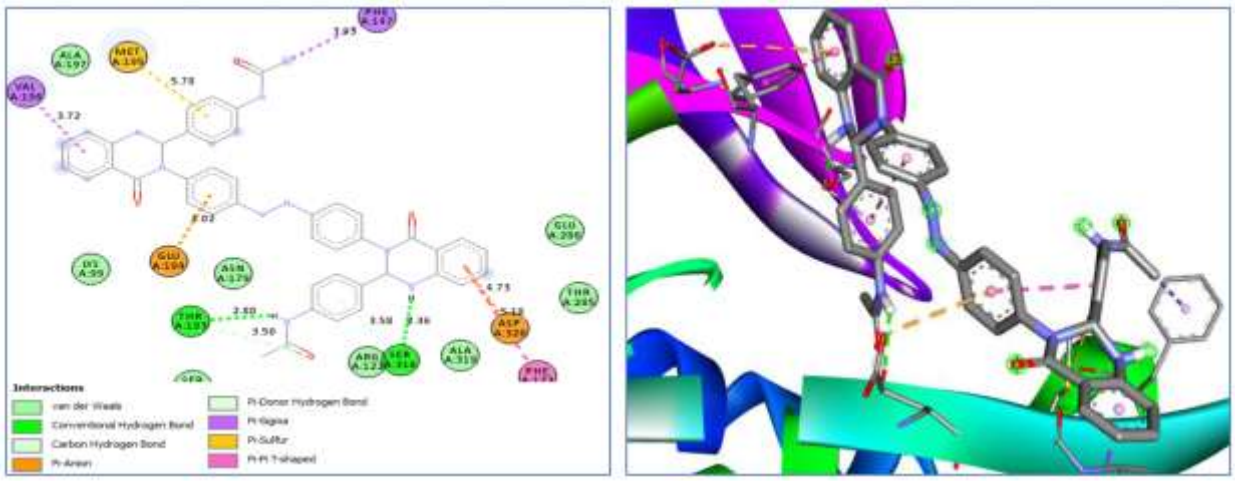

Figure 25. Three-dimensional (3D, right) and two-dimensional (2D, left) interaction diagrams of compound S_3 docked into the active site of *Pseudomonas aeruginosa* protein (PDB ID: 4DQ2).

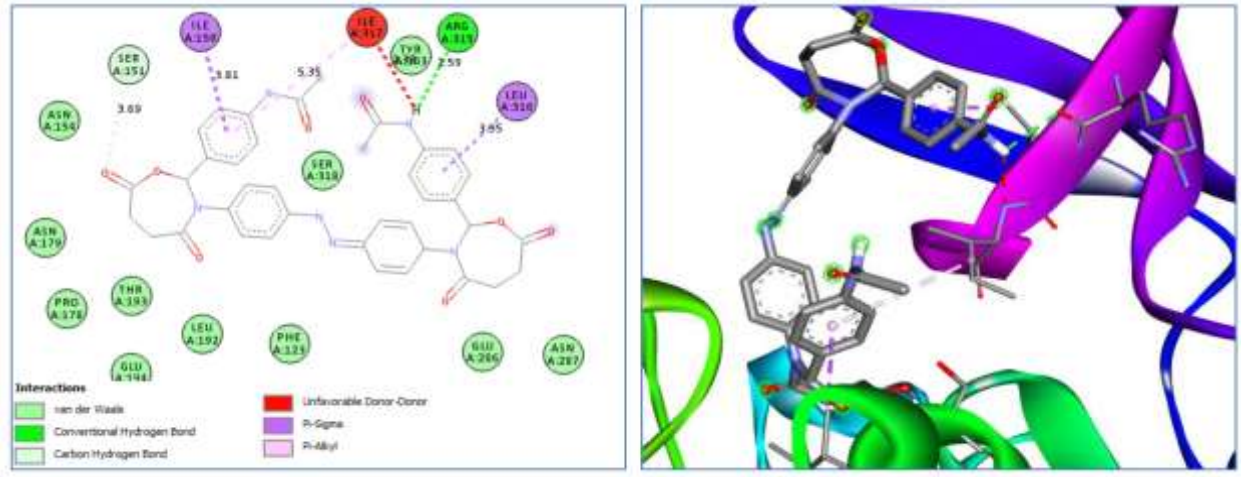

Figure 26. Three-dimensional (3D, right) and two-dimensional (2D, left) interaction diagrams of compound S_5 docked into the active site of *Pseudomonas aeruginosa* protein (PDB ID: 4DQ2).

3.5. Liquid Crystalline Properties

The liquid crystalline behavior of the synthesized compounds(S_1–S_4) wasinvestigated using polarized optical microscopy (POM). The phase transition temperatures and textures are summarized below[38,39]. The corresponding photomicrographs are presented in **Figures 27–29**.

3.5.1. Compound S_1

Compound S_1 exhibited three phase transitions upon heating. It melted at 120 °C into a smectic I phase, which cleared to an isotropic liquid at 190 °C. The transition temperatures and textures are given in **Table 4**, and representative POM images are shown in **Figure 27**.

Table 4. Phase transition temperatures for compound S_1.

Compound	Crystal (°C)	Smectic I (°C)	ΔT_{SI} (°C)
S_1	120	130	10

3.5.2. Compound S_2

Compound S_2 displayed four transitions: Cr → SmX → SmA → SmC → Iso. The phase sequence and transition temperatures are listed in **Table 5**, **Figure 28** shows the characteristic textures of the smectic phases.

Table 5: Phase transition temperatures for compound S_2.

Compound	Crystal (°C)	Smectic X (°C)	Smectic A (°C)	Smectic C (°C)	ΔT_{SA}	ΔT_{SC}
S_2	240	250	270	295	10	30

3.5.3. Compound S_3

Compound S_3 showed four transitions: Cr → SmA → N → Iso. The "marble texture" characteristic of the smectic A phase was observed. Transition data are given in **Table 6**, and POM images are shown in **Figure 29**.

Table 6. Phase transition temperatures for compound S_3.

Compound	Crystal (°C)	Smectic A (°C)	Nematic (°C)	ΔT_{SA}	ΔT_N
S_3	140	217	230	77	90

3.5.4. Compound S_4

Compound S_4 exhibited four transitions: Cr → SmA → N → Iso. The phase behavior is summarized in **Table 7**.

Table 7. Phase transition temperatures for compound S_4.

Compound	Crystal (°C)	Smectic A (°C)	Nematic (°C)	ΔT_{SA}	ΔT_N
S_4	140	240	290	100	150

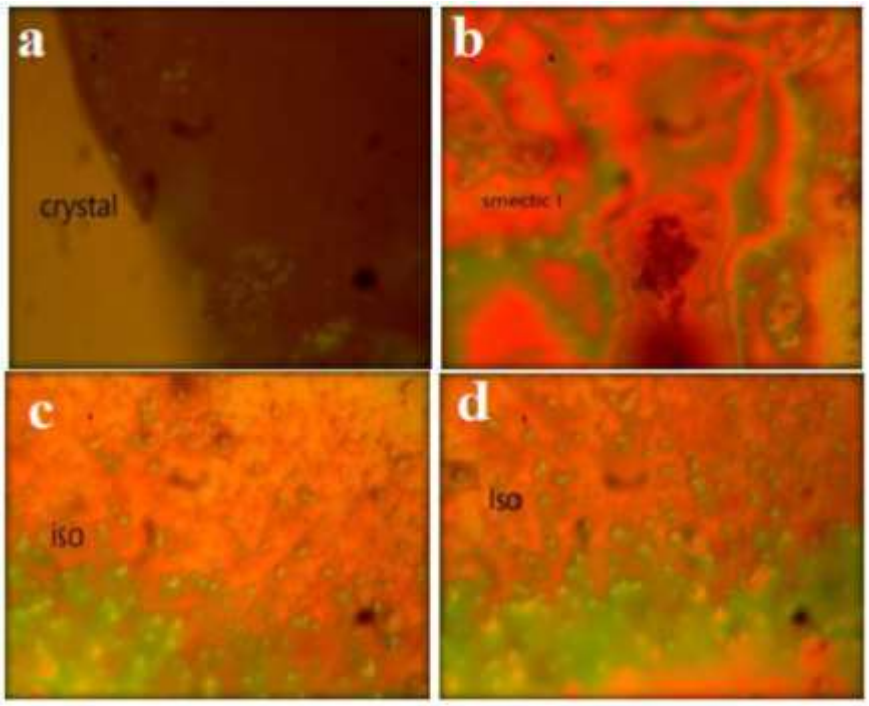

Figure 27. Polarized optical micrographs of compound S_1 at different temperatures: (a) crystalline phase at 120 °C, (b) smectic I phase at 130 °C, (c) transition to isotropic phase at 190 °C, and (d) another texture of the smectic I phase.

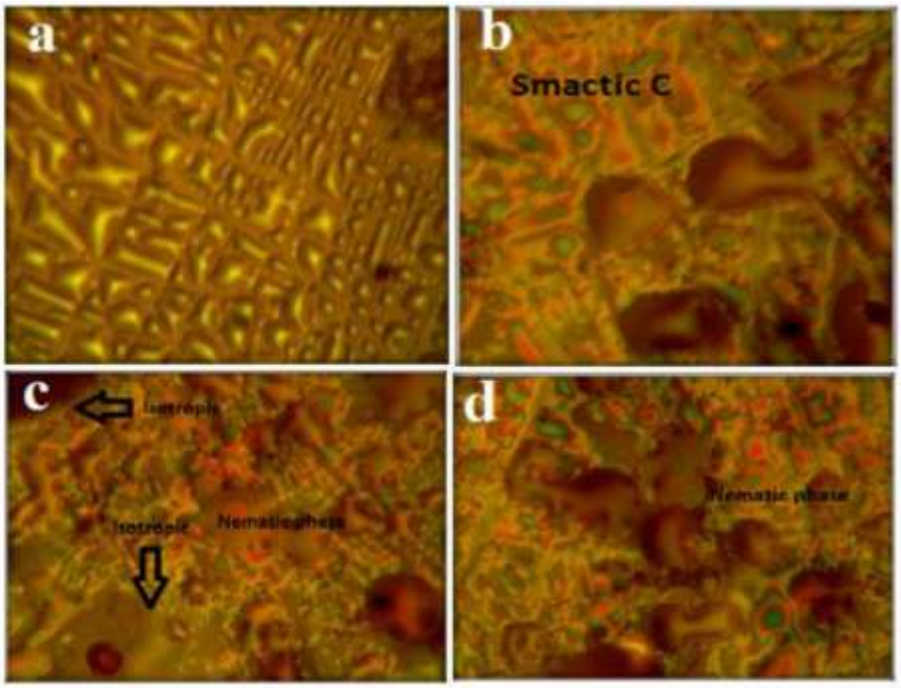

Figure 28. POM images of compound S_2 showing: (a) Smectic X phase at 250 °C, (b) Smectic A phase at 270 °C, (c) Smectic C phase at 295 °C, and (d) isotropic phase.

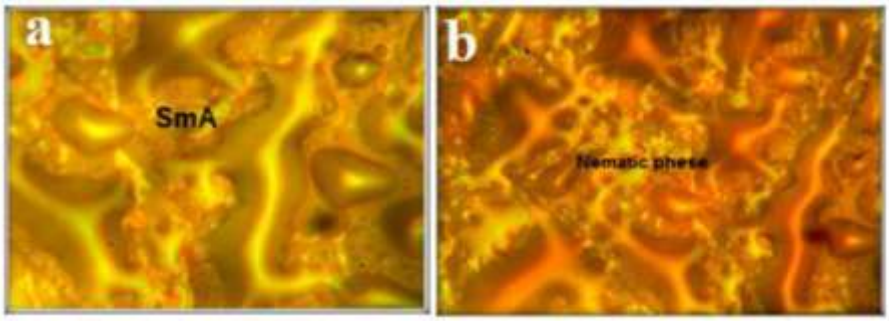

Figure 29. POM images of compound S_3: (a) smectic A phase with marble texture at 217 °C, (b) nematic phase at 230 °C.

4. Conclusion

A series of new heterocyclic compounds (S_1–S_5) were successfully synthesized via Schiff base S_1 and characterized by FT IR, ^{1}H NMR, and ^{13}C NMR spectroscopy. Antibacterial evaluation revealed that all compounds exhibited concentration dependent activity against *S. aureus* and *P. aeruginosa*. Compound S_3 showed the highest activity against *P. aeruginosa* (5 cm inhibition zone), while S_5 was most active against *S. aureus* (5 cm). Molecular docking studies supported the experimental results, showing favorable binding interactions with target proteins. Liquid crystalline studies indicated that S_1–S_4 form mesophases with wide thermal ranges, suggesting potential for materials applications. This work provides a foundation for further development of these heterocycles as antibacterial agents and functional materials.

REFERENCES

[1] Y. Zou, L. Liu, J. Liu, and G. Liu, "Bioisosteres in drug discovery: focus on tetrazole," *Future Med. Chem.*, vol. 12, no. 2, pp. 91–93, 2020. doi: 10.4155/fmc-2019-0288.

[2] A. A. Jawad, N. R. Jber, B. S. Rasool, and A. K. Abbas, "Tetrazole derivatives and role of tetrazole in medicinal chemistry: An article review," *Al-Nahrain J. Sci.*, vol. 26, no. 1, pp. 1–7, Apr. 2023. doi: 10.22401/ANJS.26.1.01.
[3] S. L. Deev, T. S. Shestakova, V. N. Charushin, and O. N. Chupakhin, "Synthesis and azido-tetrazole tautomerism of 3-azido-1, 2, 4-triazines," *Chem. Heterocycl. Compd.*, vol. 53, no. 9, pp. 963–975, Sep. 2017. doi: 10.1007/s10593-017-2153-5.
[4] V. A. Ostrovskii, R. E. Trifonov, and E. A. Popova, "Medicinal chemistry of tetrazoles," *Russ. Chem. Bull.*, vol. 61, no. 4, pp. 768–780, 2012. doi: 10.1007/s11172-012-0108-4.
[5] K. F. Sina, A. Yahyazadeh, and N. O. Mahmoodi, "Synthesis, Characterization, and Antibacterial Evaluation of 2, 3Dihydroquinazolin-4 (1H)-Ones and Some New Bis 2, 3-Dihydroquinazolin-4 (1H)- Ones Using Pre-made Pyrazole Carbaldehyde Derivatives," *Lett. Org. Chem.*, vol. 18, no. 3, pp. 176–182, 2021. doi: 10.2174/1570178617999200729192909.
[6] L. A. Dahabiyeh et al., "Molecular and metabolic alterations of 2, 3-dihydroquinazolin-4 (1 H)-one derivative in prostate cancer cell lines," *Sci. Rep.*, vol. 12, no. 1, p. 21599, 2022. doi: 10.1038/s41598-022-25681-2.
[7] E. Vessally, A. Hosseinian, L. Edjlali, A. Bekhradnia, and M. D. Esrafili, "New route to 1, 4-oxazepane and 1, 4-diazepane derivatives: synthesis from N-propargylamines," *RSC Adv.*, vol. 6, no. 102, pp. 99781–99793, 2016. doi: 10.1039/C6RA22189E.
[8] G. Y. Yeap, A. T. Mohammad, and H. Osman, "Synthesis, spectroscopic and mesomorphic studies on heterocyclic liquid crystals with 1, 3-oxazepine-4, 7-dione, 1, 3-oxazepane-4, 7-dione and 1, 3-oxazepine-1, 5-dione cores," *J. Mol. Struct.*, vol. 982, no. 1–3, pp. 33–44, 2010. doi: 10.1016/j.molstruc.2010.07.040.
[9] H. M. S. Al-Jubori, "Preparation and Characterization of Some 1, 3-Oxazepane-7, 4-Dione Derivatives and Evaluation of their Biological Activity," *Eur. J. Mod. Med. Pract.*, vol. 4, no. 4, pp. 333–343, 2024. [Online]. Available: https://www.inovatus.es/index.php/ejmmp/article/view/3066
[10] A. V. Ivanov, A. S. Bobkov, S. V. Martynovskaya, A. B. Budaev, and N. M. Vitkovskaya, "A Short-Cut to Substituted Fused Pyrrolo (2, 1-c)(1, 4) oxazines: A Hybrid Theoretical and Experimental Study," *Asian J. Org. Chem.*, vol. 12, no. 8, p. e202300153, 2023. doi: 10.1002/ajoc.202300153.
[11] M. Czyz et al., "Photocatalytic Generation of Alkyl Carbanions from Alkenes," 2023. doi: 10.26434/chemrxiv-2023-bj378.
[12] E. F. Mousa and I. K. Jassim, "Synthesis, characterization, and study the biological activity of some schiff's bases, and 1, 3-oxazepane compounds derived from sulfamethoxazole drug," *Iraqi J. Mark Res. Consum Prot.*, vol. 13, no. 1, pp. 43–54, 2021. doi: 10.28936/jmracpc13.1.2021.43.
[13] A. W. A. S. Abdul Wahed, "Preparation and Evaluation of Bacterial Activity and Study of the Crystalline Properties of Some 1,3-Oxazepine-4,7-Dione Derivatives," *Cent. Asian J. Theor. Appl. Sci.*, vol. 5, no. 2, pp. 15–26, 2024. [Online]. Available: https://cajotas.centralasianstudies.org/index.php/CAJOTAS/article/view/363
[14] H. M. S. Al-Jubori, "Preparation and Characterization of Some 1,3-Oxazepane-7,4-Dione Derivatives and Evaluation of Their Biological Activity," *Eur. J. Mod. Med. Pract.*, vol. 4, no. 4, pp. 333–343, 2024. [Online]. Available: https://www.inovatus.es/index.php/ejmmp/article/view/3066
[15] S. M. Gomha, T. A. Salaheldin, H. M. Hassaneen, H. M. Abdel-Aziz, and M. A. Khedr, "Synthesis, characterization and molecular docking of novel bioactive thiazolyl-thiazole derivatives as promising cytotoxic antitumor drug," *Molecules*, vol. 21, no. 1, p. 3, Dec. 2015. doi: 10.3390/molecules21010003.
[16] A. W. A. S. Talluh, M. J. Saleh, J. N. Saleh, and H. M. S. Al-Jubori, "Preparation, characterization, evaluation of Biological Activity, and Study of Molecular Docking of Azetidine Derivates," *Cent. Asian J. Med. Nat. Sci.*, vol. 5, no. 4, pp. 608–616, 2024. [Online]. Available: https://cajmns.centralasianstudies.org/index.php/CAJMNS/article/view/2364
[17] M. M. Aftan, A. A. Talloh, A. H. Dalaf, and H. K. Salih, "Impact para position on rho value and rate constant and study of liquid crystalline behavior of azo compounds," *Mater. Today: Proc.*, vol. 45, pp. 5529–5534, 2021. doi: 10.1016/j.matpr.2021.02.298.
[18] Y. M. A. Mohamed and Y. A. Attia, "The influence of ultrasonic irradiation on catalytic performance of ZnO nanoparticles toward the synthesis of chiral 1- substituted- 1H- tetrazolederivatives from α- amino acid ethyl esters," *Appl. Organomet. Chem.*, vol. 34, no. 9, p. e5758, 2020. doi: 10.1002/aoc.5758.
[19] S. I. Al-Khazraji, L. S. Ahamed, and R. A. Ali, "Synthesis and Characterization of some new heterocyclic derivatives from aromatic carbonyl compounds and carboxylic acids with Evaluation some of them for

biological activity," Iraqi Journal of Science, vol. 65, no. 5, pp. 2476–2488, 2024. doi: 10.24996/ijs.2024.65.5.10.
[20] S. Manzoor et al., "Tetrazole and azido derivatives of pyrimidine: synthesis, mechanism, thermal behaviour & steering of azido–tetrazole equilibrium," *ChemistrySelect*, vol. 5, no. 18, pp. 5414–5421, May 2020. doi: 10.1002/slct.202001315.
[21] M. M. Al-Tufah, S. Beebaeny, S. S. Jasim, and B. L. Mohammed, "Synthesis, Characterization of Ethyl Dioxoisoindolinyl Cyclohexenone Carboxylate Derivatives from Some Chalcones and its Biological Activity Assessment," Chemical Methodologies, vol. 7, no. 5, pp. 408–418, 2023. doi: 10.22034/chemm.2023.376779.1623.
[22] G. Su et al., "A bifunctional iminophosphorane squaramide catalyzed enantioselective synthesis of hydroquinazolines via intramolecular aza-Michael reaction to α,β-unsaturated esters," *Chem. Sci.*, vol. 12, no. 17, pp. 6064–6072, 2021. doi: 10.1039/D1SC00785A.
[23] A. H. Kshash, "Synthesis and Characterization of Tetrachloro- 1, 3-Oxazepine Derivatives and Evaluation of Their BiologicalActivities," *Acta Chim. Slov.*, vol. 67, no. 1, pp. 113–118, 2020. doi: 10.17344/acsi.2019.5162.
[24] A. H. Dalaf and F. H. Jumaa, "Synthesis, Characterization of some 1,3-Oxazepane -4,7-Dione by Traditional and Microwave routes method and evaluation of their biological activity," *Al-Utrohafor Pure Sci.*, no. 8, pp. 93–108, 2018.
[25] K. Oshimoto, B. Zhou, H. Tsuji, and M. Kawatsura, "Synthesis of substituted benzo (b)(1, 4) oxazepine derivatives by the reaction of 2-aminophenols with alkynones," *Org. Biomol. Chem.*, vol. 18, no. 3, pp. 415–419, 2020. doi: 10.1039/C9OB02639A.
[26] M. I. Khalil, "Synthesis and characterization of new oxazepine compounds derived from guanine," *Mater. Today: Proc.*, vol. 45, pp. 4960–4963, 2021. doi: 10.1016/j.matpr.2021.01.389.
[27] M. J. Saleh, J. N. Saleh, and K. Al-Badrany, "PREPARATION, CHARACTERIZATION, AND EVALUATION OF THE BIOLOGICAL ACTIVITY OF PYRAZOLINE DERIVATIVES PREPARED USING A SOLID BASE CATALYST," *Eur. J. Mod. Med. Pract.*, vol. 4, no. 7, pp. 25–32, 2024. [Online]. Available: https://www.inovatus.es/index.php/ejmmp/article/view/3519
[28] J. N. Saleh and A. Khalid, "Synthesis, characterization and biological activity evaluation of some new pyrimidine derivatives by solid base catalyst AL2O3-OBa," *Cent. Asian J. Med. Nat. Sci.*, vol. 4, no. 4, pp. 231–239, 2023. [Online]. Available: https://cajmns.centralasianstudies.org/index.php/CAJMNS/article/view/1732
[29] Y. K. Alasadi, F. H. Jumaa, A. H. Dalaf, S. M. Shawkat, and M. G. Mukhlif, "Synthesis, Characterization, and Molecular Docking of New Tetrazole Derivatives as Promising Anticancer Agents," *J. Pharm. Negat. Results*, vol. 13, no. 3, pp. 513–522, 2022. doi: 10.47750/pnr.2022.13.03.078.
[30] M. J. Saleh and K. A. Al-Badrany, "Preparation, characterization of new 2-oxo pyran derivatives by AL2O3-OK solid base catalyst and biological activity evaluation," *Cent. Asian J. Med. Nat. Sci.*, vol. 4, no. 4, pp. 222–230, 2023. [Online]. Available: https://cajmns.centralasianstudies.org/index.php/CAJMNS/article/view/1731
[31] A. W. A. Sattar Talluh, J. N. Saleh, M. J. Saleh, and H. M. Saleh Al-Jubori, "Preparation and Characterization of New Imidazole Derivatives Derived From Hydrazones and Study of their Biological and Laser Efficacy," *Cent. Asian J. Theor. Appl. Sci.*, vol. 5, no. 4, pp. 202–211, 2024. [Online]. Available: https://cajotas.centralasianstudies.org/index.php/CAJOTAS/article/view/560
[32] A. W. A. S. Talluh, M. J. Saleh, J. N. Saleh, and H. M. S. Al-Jubori, "Synthesis and Characterization of Some New Imine Graphene Derivatives and Evaluation of Their Biological Activity," *Cent. Asian J. Med. Nat. Sci.*, vol. 5, no. 4, pp. 272–290, 2024. [Online]. Available: https://cajmns.centralasianstudies.org/index.php/CAJMNS/article/view/2554
[33] F. M. Muhammad, B. A. Khairallah, and K. A. Albadrany, "Synthesis, characterization and Antibacterial Evaluation of Novel 1, 3-Oxazepine Derivatives Using A Cycloaddition Approach," *J. Angiother.*, vol. 8, no. 3, pp. 1–5, 2024. doi: 10.25122/jat-2023-0041.
[34] H. B. Howsaui, A. S. Basaleh, M. H. Abdellattif, W. M. Hassan, and M. A. Hussien, "Synthesis, structural investigations, molecular docking, and anticancer activity of some novel Schiff bases and their uranyl complexes," *Biomolecules*, vol. 11, no. 8, p. 1138, Aug. 2021. doi: 10.3390/biom11081138.
[35] A. Al-Mulla, "A review: biological importance of heterocyclic compounds," *Der Pharma Chemica*, vol. 9, no. 13, pp. 141–147, 2017. [Online]. Available: https://www.derpharmachemica.com/pharma-chemica/abstract.php?vol=9&issue=13&year=2017&month=July&aid=4750

[36] S. S. Saleh, S. S. AL-Salihi, and I. A. Mohammed, "Biological activity Study for some heterocyclic compounds and their impact on the gram positive and negative bacteria," *Energy Procedia*, vol. 157, pp. 296–306, Jan. 2019. doi: 10.1016/j.egypro.2018.11.194.
[37] A. K. Allamy and S. A. Mejbel, "Preparation, characterization and biological activity of some new seven-membered heterocyclic compounds," *World J. Adv. Res. Rev.*, vol. 15, no. 1, pp. 662–678, 2022. doi: 10.30574/wjarr.2022.15.1.0753.
[38] A. K. Amine and N. H. Karam, "Synthesis, Characterization, and Study of Liquid Crystals Properties of New Five Heterocyclic Compounds," *Ibn AL-Haitham J. Pure Appl. Sci.*, vol. 38, no. 2, pp. 194–203, Apr. 2025. doi: 10.30526/38.2.3330.
[39] A. J. Ali and N. H. Karam, "Synthesis and Characterization of Heterocyclic Compounds-Based Liquid Crystals," *Ibn AL-Haitham J. Pure Appl. Sci.*, vol. 36, no. 3, pp. 1–3, 2023. doi: 10.30526/36.3.3096.